Original Research Article

Adsorption Thermodynamics, kinetics and mechanism for the adsorption of Erythromycin onto Multi-Walled Carbon Nanotubes

ABSTRACT
The ability of multi-walled carbon nanotubes (MWCNT) to adsorb Erythromycin antibiotic from aqueous solution has been investigated through batch experiments. The adsorption of Erythromycin onto MWCNT has been found to depend on adsorbent dose, initial concentration and contact time. The experiments were carried out at natural solution pH. The experiments showed that the highest removal rate was 99.4% under optimal conditions. The adsorption kinetic results showed that the pseudo-second order model was more suitable to explain the adsorption of Erythromycin onto MWCNT. The adsorption mechanism results showed that the adsorption process was controlled by both the internal and external diffusion of Erythromycin molecules. The values of free energy change (ΔG^0) and enthalpy change (ΔH^0) indicated the spontaneous, feasible, and endothermic nature of the adsorption process.

Keywords: Batch adsorption; MWCNT; Erythromycin; Kinetic; Thermodynamics.

1. INTRODUCTION

In recent years, antibiotics have been recognized as one of the most important water contaminants [1, 2]. Antibiotics are designed specifically as a drug to treat or prevent infective diseases in human or animal body [3, 4]. The use of antibiotics has become an indispensable in human life and the global market consumption of these drugs increase steadily every year [5, 6]. For preventing or treating infections in humans or animals, only some parts of the antibiotics given dose are metabolized and the rest are excreted still as active compound [7, 8]. The abuse of antibiotics leaded to the emergence and persistence of resistant strains, which could become a serious public health crisis in the future [9, 10]. Antibiotics have been found in the water environment, including in waste water, seawater treatment plants, surface water, ground water, and even in drinking water [11].

Erythromycin is a 14-carbon macrolide produced by fermentation of Streptomyces erythreus. It is a broad-spectrum polyketide antibiotic, specially indicated in the treatment of respiratory and skin complains [12]. It has a similar activity spectrum to penicillin and is used by penicillin-sensitive people to combat Gram-positive bacteria. In addition it is used against Mycoplasma, Campylobacter and Legionella [13].

The removal of antibiotics from pharmaceutical wastewater is quite expensive; however this wastewater must be treated properly prior to the release into environment [14]. Among the available process for the treatment of wastewater containing antibiotics, the adsorption process is considered as the most effective and efficient method [15, 16].

Adsorption is gaining wider acceptance for large-scale separation from liquid due to the low energy nature of adsorptive separation processes when compared to other operations namely

distillation or solvent extraction from diluted aqueous solutions [17, 18]. Adsorption is a physical–chemical process that involves the mass transfer of a solute (adsorbate) from the fluid phase to the sorbent surface till the thermodynamic equilibrium of the adsorbate concentration is attained, with no further net adsorption [19].

Carbon Nanotubes (CNTs) have been studied extensively in last decade for different applications including water purification due to their extraordinary physiochemical properties associated with their small size, tubular morphology and ease of functionalization [20]. CNTs have been used for removal of antibiotics, dyes and heavy metals from its aqueous solution [21-23].

The main objective of this work is to study the adsorption potential of MWCNT for the removal of Erythromycin from aqueous solution. The effects of several operating parameters such as adsorbent dose, initial Erythromycin concentration, mixing rate, contact time, and temperature on the Erythromycin adsorption at fixed pH=7 were investigated. The adsorption behavior of MWCNT towards Erythromycin removal was studied using kinetics and thermodynamic viewpoints.

2. MATERIALS AND METHODS

The multi-wall carbon nanotubes (MWCNT) used in this study was of more than 98% purity and provided from Research Institute of Petroleum Industry (RIPI), Tehran, Iran). The size and morphology of MWCNT were examined by scanning electron microscope (JEOL JSM 6500F) and transmission electron microscopy (TEM) (using a Philips XL30).
Erythromycin (Fig. 1) a antibiotic, with a molecular formula of $C_{37}H_{67}NO_{13}$, molecular weight 733.93, λ_{max} of 280 nm, and C.I. number of 114-07-8, was chosen as a model antibiotic for the present experimental studies. The stock solution of Erythromycin (500 mg/L) was prepared by dissolving 500 mg of Erythromycin powder in 1000 mL of distilled water. The stock solution was diluted with distilled water accordingly to obtain solutions of desired concentrations (10–100 mg/L).

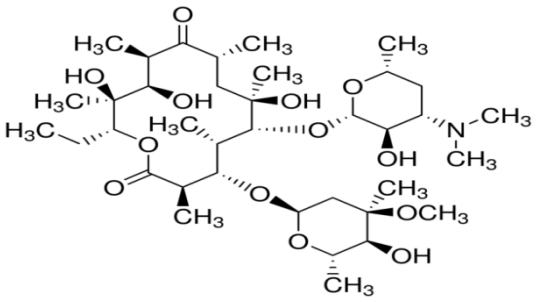

Fig 1. Chemical structure of Erythromycin

Batch Adsorption Test and Optimized Conditions

The adsorption experiment was carried out as batch inside 250 mL Erlenmeyer flasks containing 100 mL of synthetic Erythromycin solution. Initial pH of the samples was set by 0.1 molar NaOH and HCl. Afterwards; 0.4 g/L of adsorbent were added up to the solutions with Erythromycin initial concentration of 25 ppm. The final solution was stirred at 30 °C and 120 rpm for 75 min. The solutes were filtered through filter paper and 5 mL of the solution was analyzed to measure adsorbed Erythromycin ion concentration. The

optimization process repeated for other parameters as well as contact time. These parameters were adsorbent dosage (0.1–1 g/L), mixing rate (0–200 rpm), and initial concentration of Erythromycin ion in the solution (10–100 ppm). The contact time of the solution was adjusted to optimum condition and one of the parameters considered variable while others were constant. The optimized condition of each parameter was selected and the investigation continued to define the optimum condition of other parameters. The Erythromycin concentration was identified by sphectrophotometry at 280 nm (model DR-5000). In this research, all of the tests performed twice and the best results were reported.
The amount of adsorbed ions by adsorbent for each gram of adsorbent is identified by following Eq [23, 24]:

$$q_e = \frac{(C_0 - C_e)}{W} \times V$$

Where q_e is the amount of adsorbed material per gram of MWCNT (mg/g) in the equilibrium state, C_0 and C_e are initial and equilibrium concentrations of Erythromycin (mg/L), V is the solution volume and W is the weight of the MWCNT.

3. RESULTS AND DISCUSSION

Fig. 2 displays the surface morphology of MWCNTs. The SEM and TEM figures show that the MWCNTs were cylindrical and the range of main external and internal diameters was 2-3.5 and 1.2-1.7 nm, respectively. The specific surface area of the adsorbent used in this study was 782.8 m^2/g.

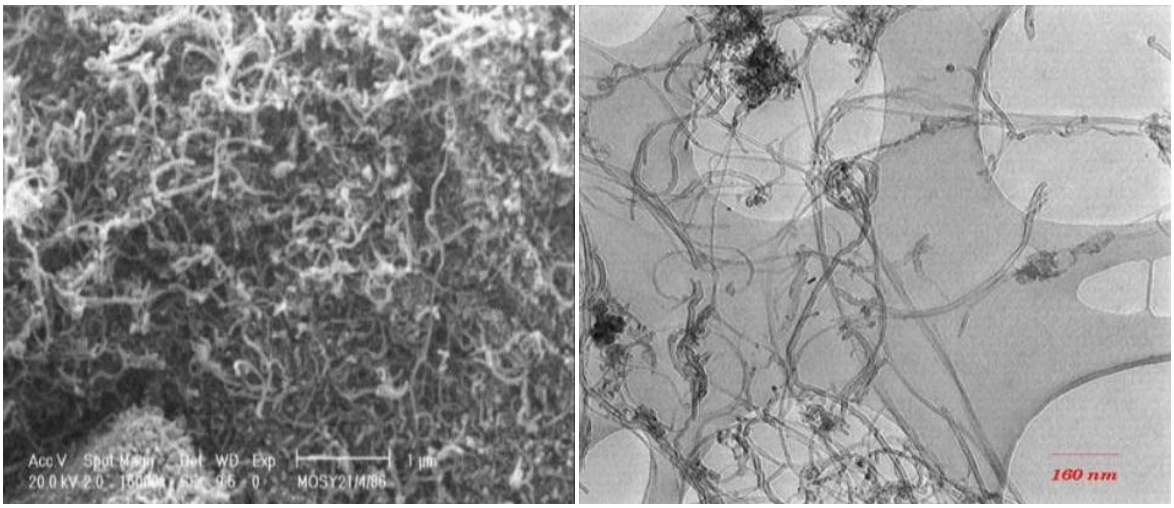

Fig. 2. Micrographs of MWCNTs (a) SEM and (b) TEM.

Effect of contact time and temperature: In order to establish the equilibrium time for Erythromycin adsorption onto MWCNT, contact time influence over the process evolution was investigated until equilibrium reached. As shown in Fig. 3 the removal efficiency increases rapidly (in the first 75 min) due to the abundant availability of active binding site of the adsorbent and then remained almost constant with the occupancy of these sites [25-27]. Further increase in contact time did not enhance the adsorption; therefore the contact time was selected 75 min for further experiments (equilibrium).

The effect of temperature on adsorption of Erythromycin onto MWCNT was conducted at 15, 25, 35 and 45 ℃ (288-318 K). Results presented in Fig. 3 and showed that the adsorption increases significantly with the increase in temperature from 288 K (adsorption capacity= 104.8 and removal efficiency= 83.71%) to 318 K (adsorption capacity= 124.6 and removal efficiency= 99.68%), indicating that the biosorption process is endothermic. The increase in the adsorption capacity with temperature may be attributed to either change in pore size of the adsorbent improving intra-particle diffusion within the pores or enhancement in the chemical affinity of Erythromycin to the surface of the adsorbent [28]. This leads to increased disorder at the MWCNT surface and intensification of chemical interactions that take place during the adsorption process which have as a result an increase in adsorption capacity [29, 30].

Effect of Mixing Rate: The mixing rate and turbulence making inside aqueous solution is an important parameter in adsorption process as disturbance increases the possibility of contact between the adsorbent and ions which results in higher recovery. In order to examine mixing rate on adsorption process, the parameters were determined in laboratory conditions as mixing rate 0–200 rpm, initial Erythromycin 100 ppm, time 75 min, temperature 30 °C, adsorbent dosage 0.8 g/L and pH = 7. The magnetic mixer was used for mixing process and this parameter effect is shown in Fig. 4. According to the Fig. 4, increasing the mixing rate in the range of 0–200 rpm increases the recovery of Erythromycin adsorption by the adsorbent. Higher mixing rate means higher contact possibility between active sites and Erythromycin ions [30, 31]. The optimum removal was at 200 rpm mixing rate equal to 98.9%.

Effect of Adsorbent Dose: The amount of used adsorbent is a significant parameter in adsorption process, as it determines the adsorption capacity in a certain concentration of adsorbed material. The testing parameters for the range of MWCNT dosage (0.2–2 g/L) to remove Erythromycin are initial concentration 100 ppm, temperature 30 °C, contact time 75 min, mixing rate 200 rpm, pH = 7. Fig 5 shows the effect of MWCNT dose on adsorption of Erythromycin. The findings revealed that increasing the amount of used adsorbent leads to increase in Erythromycin adsorption, as higher dosage increases the number of active sites for Erythromycin ion adsorption [32, 33]. Increase in the amount of adsorbent up to 1 g/L, results in the higher adsorption of Erythromycin removal that is 92.7% . Higher dosages of adsorbent in aqueous solution, more than 1 g/L, show a negligible increase in adsorption because of saturation inactive sites [34]. Even in some cases the final adsorption is reduced as there was the higher possibility of contact between adsorbent particles and active sites and this factor makes flocculation on the sites and ultimately decreases the number of active sites and adsorbent surfaces and final recovery as a result.

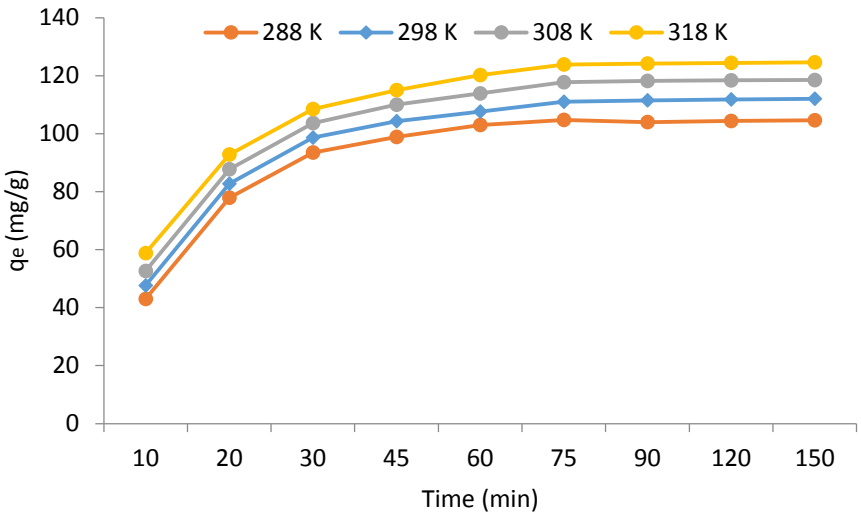

Fig 3. Effect of contact time and temperature on Erythromycin removal (pH =7, Adsorbent dosage 0.8 g/L, mixing rate 200 rpm, C_0 = 100 mg/L)

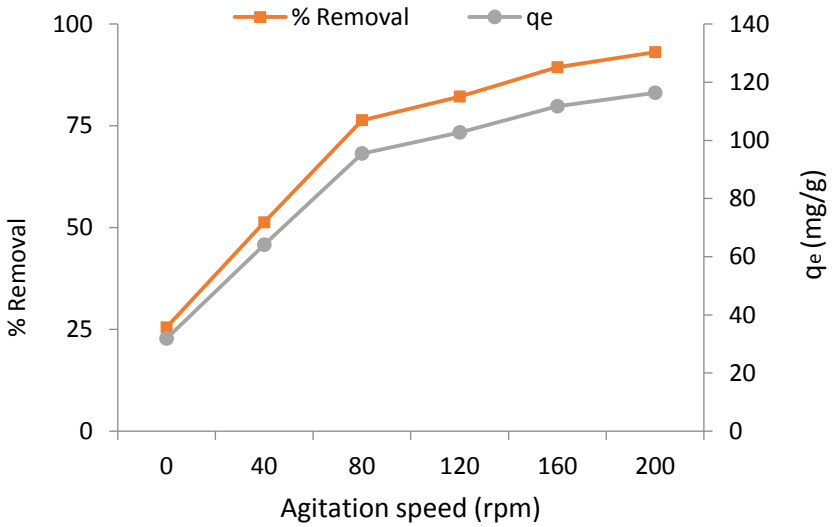

Fig. 4. Effect of mixing rate on Erythromycin adsorption (C_0 = 100 mg/L, temp= 25± 2◦C, time 75 min, adsorbent dosage 0.8 g/L, pH = 7)

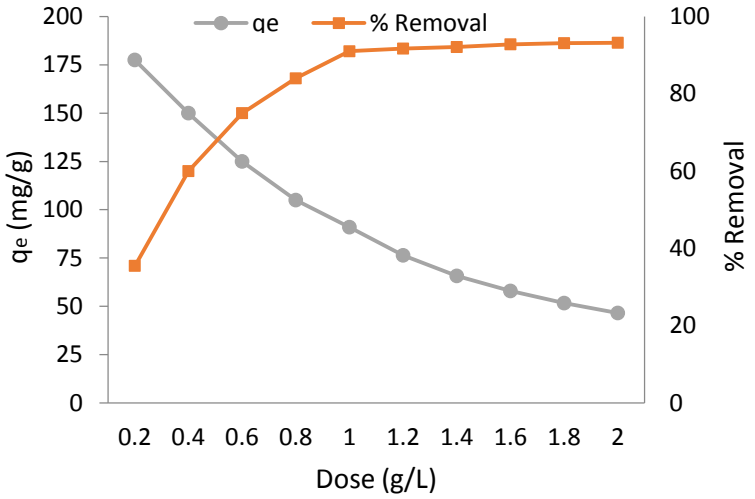

Fig 5: Effect of adsorbent dosage on Erythromycin adsorption (C_0 = 100 mg/L, time = 75 min, pH = 7, temp= 25 ± 2◦C and mixing rate 200 rpm)

Adsorption thermodynamics

The thermodynamics for Erythromycin removal by sesame was investigated in temperature range of 288-318 K, and the influence of temperature on the adsorption capacity is shown in Fig. 3. It can be found that there is an increase in the adsorption capacity of sesame with the temperature increase. Thermodynamic parameters such as change in Gibbs free energy (ΔG^0), enthalpy (ΔH^0) and entropy (ΔS^0) were determined using the following equation [34, 35]:

$K = q_e / C_e$

$\Delta G = - RT \ln K$

$$\ln K = \frac{\Delta S^0}{R} - \frac{\Delta H^0}{RT}$$

Table 1 summarizes the thermodynamic parameters associated the adsorption process. Values of ΔG^0 were calculated from the values of adsorption equilibrium constant (K) using above equations. The negative values of ΔG^0 at the three temperatures show that the adsorption process is spontaneous and the degree of spontaneity increases with increasing the temperature [36, 37]. The values of ΔH^0 and ΔS^0 are calculated from the slope and the intercept of the linear plot of Ln K vs. 1/T. The overall adsorption process seems to be endothermic (ΔH^0= 76.25 KJ/mol). This result also supports the suggestion that the adsorption capacity of sesame increases with increasing temperature. Table 1 also shows that the ΔS^0 value is positive (entropy increases as a result of adsorption). A positive ΔS^0 value reflects the affinity of the adsorbent to the Erythromycin, as a result of redistribution of energy between the adsorbate and adsorbent [38]. Before adsorption occurs, the Erythromycin near the surface of the MWCNT will be more ordered than in the subsequent adsorbed state and the ratio of free Erythromycin ions to ions interacting with the adsorbent will; be higher in the adsorbed state.

Table 1: Thermodynamic parameters of the Erythromycin adsorption onto MWCNT			
T (K)	ΔG° (kJ mol^{-1})	ΔS° (J mol^{-1} K^{-1})	ΔH° (kJ mol^{-1})
288	-4.54	0.277	76.25
298	-5.71		
308	-8.24		
318	-13.11		

Adsorption kinetics

The adsorption n of Erythromycin on MWCNT versus equilibrium time is presented in Fig. 3. It is found that the adsorption kinetics of Erythromycin onto MWCNT included two steps: a fast initial adsorption followed by a slow gradual adsorption. The initial rapid phase (first (30 min) accounted for a considerable portion of the adsorption. During this stage, about 80% of Erythromycin was adsorbed, which can be attributed to the rapid diffusion of Erythromycin ion from solution to the external surface of MWCNT. Adsorption in the subsequent time was slower and probably resulted from the diffusion of metal ions into the porous structures of the adsorbent.
To evaluate the differences in the adsorption kinetic rates, the pseudo-first-order, pseudo-second-order, intraparticle diffusion and Boyd models were used to fit the results.

The pseudo-first-order kinetic model is generally expressed as follows [39, 40]:

$$\log (q_{e-} q_t) = \log q_e - \frac{K}{2.303} t$$

Where q_e is the amount of Erythromycin adsorbed per unit mass of MWCNT at equilibrium (mg/g), q_t is the amount of Erythromycin adsorbed per unit mass of MWCNT at any time t (mg/g), t is the time (min), and K is the pseudo-first-order rate constant (1/min). The values of K and q_e were estimated from the slope and intercept of the linear plot of log (q_e-q_t) versus t (Fig 6a), and these values are listed in Table 2.

The pseudo-second-order kinetic model is given as follows [41, 42]:

$$\frac{t}{q_t} = \frac{1}{K_2}\frac{1}{q_e^2} + \frac{1}{q_e} t$$

Where K_2 is the pseudo-second-order rate constant (g/mg.min) and $K_2.q^2_e$=h is the initial adsorption rate (mg/g.min). The values of K_2 and q_e were estimated from the slope and intercept of the linear plots of t/q_t versus t (Fig 6b), and the values are listed in Table 2.

The calculated q_e values for all the studied initial Erythromycin concentrations from the pseudo-first-order kinetic model differed appreciably from the experimental q_e values. However, in the pseudo-second-order kinetic model the calculated q_e values were very close to the experimental qe values for all the studied initial Erythromycin concentrations. Further, the obtained coefficient of determination (R^2) values of the pseudo-second-order kinetic model are higher than the obtained R^2 values of the pseudo-first-order kinetic model, indicating that the pseudo-second-order kinetic model better obeys the adsorption kinetic data than the pseudo-first-order kinetic model.

Intraparticle diffusion model

The intraparticle diffusion equation is given as [43, 44]:

$q_t = K\, t^{0.5} + C$

Where q_t is the amount of solute on the surface of the sorbent at time t (mg/g) and K is the intraparticle diffusion rate constant (mg/g.min$^{1/2}$). If intraparticle diffusion is the rate-limiting step in the adsorption of Erythromycin onto MWCNT, then the plot of qt versus $t^{1/2}$ should be a straight line and pass through the origin. The deviation of the plot of q_t versus $t^{1/2}$ from linearity indicates that the rate-limiting step should be film diffusion controlled. It was observed from Figure 6C that the plots consist of two linear portions: the first linear portion is due to film diffusion and the second is due to intraparticle diffusion. The straight line does not pass through the origin, therefore, intraparticle diffusion is not only the rate-limiting step, and film diffusion control may be involved in the adsorption process. The values of K and C were estimated from the slope and intercept of the plot of q_t versus $t^{1/2}$, and the constants of the intraparticle diffusion model are presented in Table 2 with R^2 values.
The dual nature of the intraparticle diffusion plot (Fig 6 C) confirms the presence of both film and intraparticle diffusion. In order to predict the actual slowest step in the adsorption process, the adsorption kinetic data were further analyzed using the Boyd kinetic model. The Boyd kinetic expression is given as [45, 46]:

$$F = \frac{q_t}{q_e} = 1 - \frac{6}{\pi^2} \exp(-Bt)$$

Equation can be modified and rearranged into the following form of the expression [47-49]:

$$B = -0.4977 - \mathrm{Ln}(1-F) \qquad F = \frac{q_t}{q_e}$$

Where q_e is the amount of adsorbate adsorbed at infinite time (mg/g) and q_t represents the amount of Erythromycin adsorbed at any time t (min), F represents the fraction of solute adsorbed at any time t, and B is a mathematical function of F. The B values at different contact times can be calculated using equation above for various time intervals. The calculated B values were plotted against time t.
Figure 6d is used to identify whether film diffusion or intraparticle diffusion controls the overall rate of the adsorption process. If the plots of [(0.4977 – Ln (1-F) or B versus time t] are linear and pass through the origin, then the actual slowest step in the process of the adsorption of Erythromycin onto MWCNT is intraparticle diffusion. From Figures 6d, it was observed that the plots are linear but do not pass through the origin, which confirms that film diffusion mainly control the adsorption process.

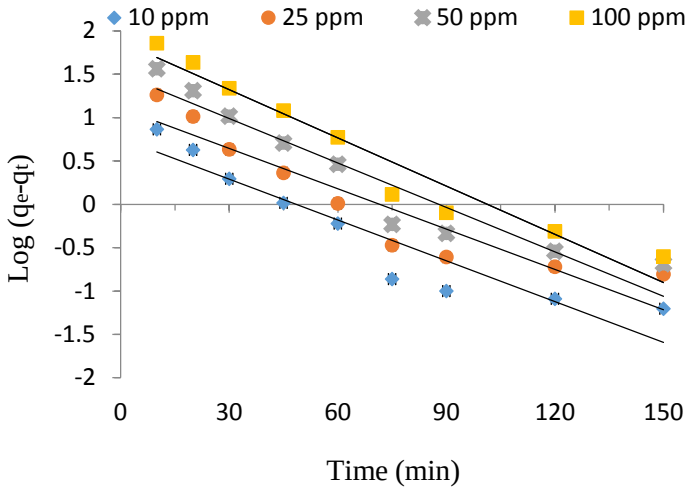
10 ppm
25 ppm
50 ppm
100 ppm
Log (qe-qt)
Time (min)

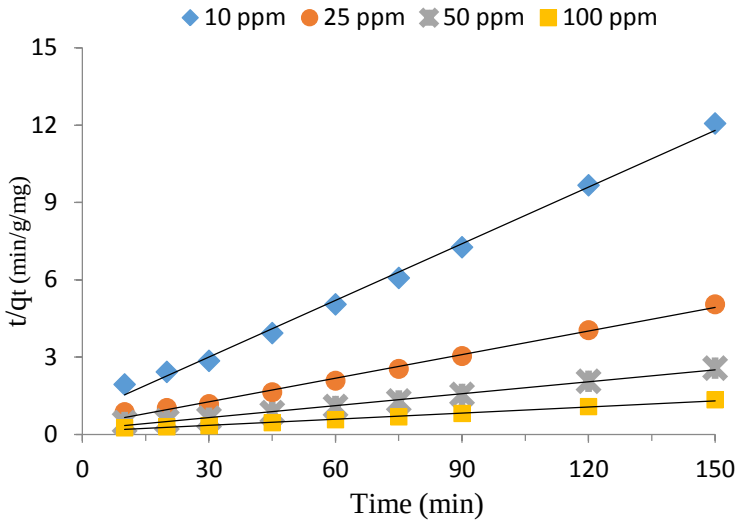
10 ppm
25 ppm
50 ppm
100 ppm
t/qt (min/g/mg)
Time (min)

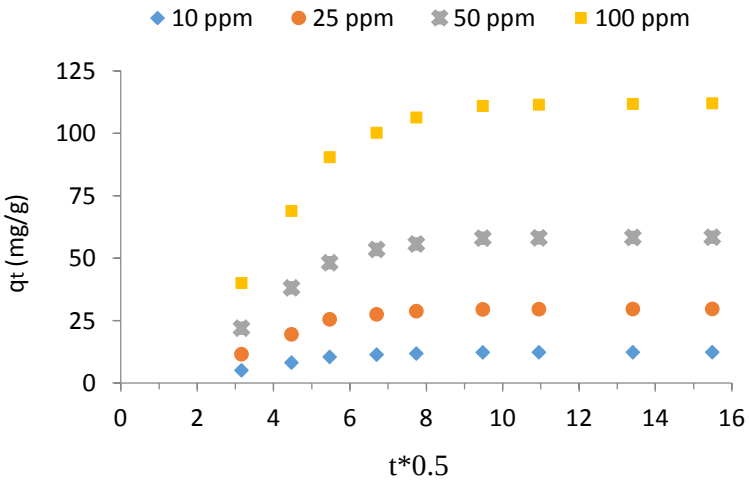
10 ppm
25 ppm
50 ppm
100 ppm
qt (mg/g)
t*0.5

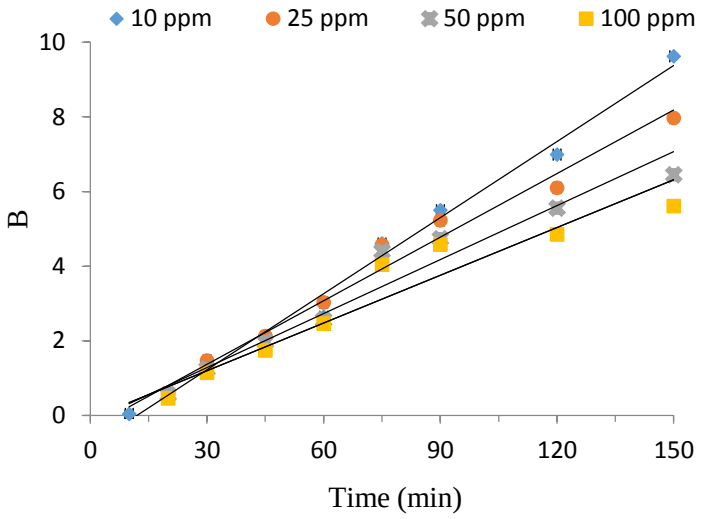

Fig. 6. Kinetic plots for the adsorption of Erythromycin onto MWCNT a: Pseudo-first order b: Pseudo-second order C: Intraparticle diffusion d: Boyd model

Table 2: Kinetic parameters for the adsorption of Erythromycin onto MWCNT at various concentration

C_o (mg/L)	q_e (exp) mg/g	Pseudo-first order			Pseudo-second order			Intraparticle diffusion			Boyd
		K_1	q_e	R^2	K_2	q_e	R^2	K	C	R^2	R^2
10	12.43	0.024	4.91	0.892	0.0066	13.69	0.995	0.464	6.80	0.741	0.972
25	29.75	0.031	9.17	0.874	0.0026	33.33	0.993	1.13	16.11	0.756	0.956
25	58.44	0.034	25.16	0.909	0.0011	66.65	0.994	2.32	30.27	0.723	0.949
100	125.05	0.036	52.71	0.942	0.0004	142.8	0.993	4.73	54.33	0.784	0.962

4. CONCLUSION

The adsorption kinetics and thermodynamics of Erythromycin on MWCNT were studied. The sorption of Erythromycin on MWCNT was rapid during the first 30 min and the equilibrium attained within 75 min. The kinetic processes of Erythromycin adsorption were described by applying pseudo-first-order, pseudo-second-order, Intraparticle diffusion and Boyd models. The kinetic data for the adsorption process obeyed a pseudo-second-order kinetic model, suggesting that the adsorption process is chemisorption. The MWCNT investigated in this study showed good potential for the removal of Erythromycin from aqueous solution

REFERENCES

1. Balarak D, Mahdavi Y, Maleki A, Daraei H and Sadeghi S. Studies on the Removal of Amoxicillin by Single Walled Carbon Nanotubes. British Journal of Pharmaceutical Research. 2016;10(4): 1-9.
2. Putra EK, Pranowoa R, Sunarsob J, Indraswatia N, Ismadjia S. Performance of activated carbon and bentonite for adsorption of amoxicillin from wastewater: mechanisms, isotherms and kinetics. Water Res. 2009; 43, 2419-2430.
3. Adrianoa WS, Veredasb V, Santanab CC, Gonçalves LRB. Adsorption of amoxicillin on chitosan beads: Kinetics, equilibrium and validation of finite bath models. Biochemical Engineering Journal. 2005; 27(2) ;132-37.
4. Balarak D, MahdaviY and Mostafapour FK. Application of Alumina-coated Carbon Nanotubes in Removal of Tetracycline from Aqueous Solution. British Journal of Pharmaceutical Research.2016; 12(1): 1-11.

5. Chen WR, Huang CH. Adsorption and transformation of tetracycline antibiotics with aluminum oxide. Chemosphere. 2010; 79, 779–785.
6. Xu L, Pan J, Dai J, Li X, Hang H, Cao Z, Yan Y. Preparation of thermal-responsive magnetic molecularly imprinted polymers for selective removal of antibiotics from aqueous solution. Journal of Hazardous Materials. 2012; 233-234;48-56.
7. Alexy R, Kumpel T, Kummerer K. Assessment of degradation of 18 antibiotics in the closed bottle test. Chemosphere. 2004 ; 57, 505–512.
8. Balarak D, Azarpira H, Mostafapour FK. Study of the Adsorption Mechanisms of Cephalexin on to AzollaFiliculoides. Der Pharma Chemica, 2016, 8(10):114-121
9. Balarak D, Mostafapour FK, Joghataei A. Experimental and Kinetic Studies on Penicillin G Adsorption by Lemna minor. British Journal of Pharmaceutical Research. 2016; 9(5): 1-10.
10. Choi KJ, Kim SG, Kim SH. Removal of antibiotics by coagulation and granular activated carbon filtration. J. Hazard. Mater. 2008; 151;38–43.
11. Fatta-Kassinos D, Meric S, Nikolau A. Pharmaceutical residues in environmental waters and wastewater: current state of knowledge and future research, Anal. Bioanal. Chem. 2011; 399; 251-275.
12. Maria HL, Ribeiro E, Isabel AC. Modelling the adsorption kinetics of erythromycin onto neutral and anionic resins. Bioprocess Biosyst Eng. 2003; 26: 49–55.
13. Balarak D, Mostafapour FK, Bazrafshan E, Saleh, TA. Studies on the adsorption of amoxicillin on multi-wall carbon nanotubes.Water science and technology. 2017; 75(7); 1599-1606
14. Balarak D, Mostafapour FK. Batch Equilibrium, Kinetics and Thermodynamics Study of Sulfamethoxazole Antibiotics Onto Azolla filiculoides as a Novel Biosorbent. British journal of pharmaceutical research. 2017;13(2); 1-11.
15. Balarak D, Mostafapour FK, Khatibi AD. Nonlinear Isotherms and Kinetics and Application Error Functions for Adsorption of Tetracycline on Lemna Minor. British journal of pharmaceutical research. 2018;23(2); 1-11.
16. Yu F, Li Y, Han S, Jie Ma J. Adsorptive removal of antibiotics from aqueous solution using carbon Materials. Chemosphere. 2016;153;365–385.
17. Aksu Z, Tunc O. Application of biosorption for Penicillin G removal: Comparison with activated carbon. Process Biochemistry. 2005;40(2):831-47.
18. Balarak, D, Joghataei A, Mostafapour FK. Ciprofloxacin Antibiotics Removal from Effluent Using Heat-acid Activated Red Mud. British journal of pharmaceutical research. 2017; 20(5); 1-11.
19. Balarak D, Mostafapour FK, Azarpira H. kinetic and Equilibrium Studies of Sorption of Metronidazole Using Graphene Oxide. British journal of pharmaceutical research. 2017; 19 (4); 1-10.
20. Ji L, ChenW, Duan L and Zhu D. Mechanisms for strong adsorption of tetracycline to carbon nanotubes: A comparative study using activated carbon and graphite as adsorbents. Environ. Sci. Technol. 2009,43 (7), 2322–27.
21. Balarak D, Mostafapour FK, Joghtaei A. Thermodynamic Analysis for Adsorption of Amoxicillin onto Magnetic Carbon Nanotubes. British journal of pharmaceutical research. 2017; 16 (6); 1-10.
22. Azarpira H, Mahdavi Y, Khaleghi O, Balarak D. Thermodynamic studies on the removal of metronidazole antibiotic by multi-walled carbon nanotubes. Der Pharmacia Lettre. 2016; 8(11):107-13.
23. Gao J and Pedersen JA. Adsorption of Sulfonamide Antimicrobial Agents to Clay Minerals. Environ. Sci. Technol. 2005, 39(24). 9509-16.
24. Dutta M, Dutta NN,Bhattachary KG. Aqueous phase adsorption of certain beta-lactam antibiotics onto polymeric resins and activated carbon. Separation and Purification Technology.1999;16(3);213-24.
25. Peterson JW, Petrasky LJ, Seymourc MD, Burkharta RS, Schuilinga AB. Adsorption and breakdown of penicillin antibiotic in the presence of titanium oxide nanoparticles in water. Chemosphere. 2012;87(8); 911‑7.
26. Ghauch A, Tuqan A, Assi HA: Elimination of amoxicillin and ampicillin by micro scale and nano scale iron particles. Environ Pollut. 2009,157:1626–1635.

27. Balarak D, Mostafapour FK, Akbari, H. Adsorption of Amoxicillin Antibiotic from Pharmaceutical Wastewater by Activated Carbon Prepared from Azolla filiculoides. British journal of pharmaceutical research. 2017; 18(3); 1-10.
28. Balarak D, Azarpira H. Photocatalytic degradation of sulfamethoxazole in water: investigation of the effect of operational parameters. International Journal of Chem Tech Research. 2016; 9(12):731-8.
29. Balarak D, Mostafapour FK, Azarpira H. Adsorption Kinetics and Equilibrium of Ciprofloxacin from Aqueous Solutions Using Corylus avellana (Hazelnut) Activated Carbon. British journal of pharmaceutical research. 2016; 13 (3); 1-10.
30. Erşan M, Bağd E. Investigation of kinetic and thermodynamic characteristics of removal of tetracycline with sponge like, tannin based cryogels. Colloids and Surfaces B: Biointerfaces. 2013;104;75-82.
31. Banerjee SS, Chen DH. Fast removal of copper ions by gum arabic modified magnetic nano-adsorbent, J. Hazard Mater. 2007;147;792–799.
32. Qu S, Wang J, Kong J, Yang P, Chen G. Magnetic loading of carbon nanotube/nano-Fe3O4 composite for electrochemical sensing, Talanta. 2007; 71;1096–102.
33. Wu C, Adsorption of reactive dye onto carbon nanotubes: equilibrium, kinetics and thermodynamics, J. Hazard Mater. 2007;144;93–100.
34. Balarak D, Mostafapour FK. Batch Equilibrium, Kinetics and Thermodynamics Study of Sulfamethoxazole Antibiotics Onto Azolla filiculoides as a Novel Biosorbent. British journal of pharmaceutical research. 2016; 13 (2); 1-10.
35. Balarak D, Mostafapour FK, Azarpira H. Langmuir, Freundlich, Temkin and Dubinin-radushkevich Isotherms Studies of Equilibrium Sorption of Ampicilin unto Montmorillonite Nanoparticles. British journal of pharmaceutical research. 2016; 20 (2); 1-10.
36. Malakootian M, Balarak D, Mahdavi Y, Sadeghi SH, Amirmahani N. Removal of antibiotics from wastewater by azollafiliculoides: kinetic and equilibrium studies. International Journal of Analytical, Pharmaceutical and Biomedical Sciences. 2015;4(7);105-113.
37. Chung WH. Adsorption of reactive dye onto carbon nanotubes: equilibrium, kinetics and thermodynamics, J. Hazard Mater. 2007;144; 93–100.
38. Ngomsik AF, Bee A, Draye M, Cote G, Cabuil V. Magnetic nano- and microparticles for metal removal and environmental applications: a review, C. R. Chimie. 2005;8;963–70.
39. Ngomsik AF, Bee A, Cote G. Nickel adsorption by magnetic alginate microcapsules containing an extractant, Water Res. 2006;40;1848–56.
40. Ma W, Ya FQ, Han M, Wang R. Characteristics of equilibrium, kinetics studies for adsorption of fluoride on magnetic-chitosan particle, J. Hazard Mater. 2007;143;296–302.
41. Yang N, Zhu S, Zhang D, Xu S. Synthesis and properties of magnetic Fe3O4-activated carbon nanocomposite particles for dye removal. Mater. Lett. 2008; 62;645–47.
42. Peng H, Pana B, Wu M, Ran Liu R, Zhanga D, Wu D, Xing B. Adsorption of ofloxacin on carbon nanotubes: Solubility, pH and cosolvent effects. Journal of Hazardous Materials. 2012;211-212;342-48.
43. Chang PH, Li Z, Jean JS, Jiang WT, Wang CJ, Lin KH. Adsorption of tetracycline on 2:1 layered non-swelling clay mineral illite. Appl. Clay Sci. 2012; 67;158–163.
44. Balarak D, Mostafapour FK, Joghataei A. Kinetics and mechanism of red mud in adsorption of ciprofloxacin in aqueous solution. Bioscience biotechnology research communications. 2017; 10(1); 241-248.
45. Balarak D, Mostafapour F K, Joghataei A. Biosorption of amoxicillin from contaminated water onto palm bark biomass. International journal of life science and pharma research. 2017;7(1);9-16
46. Upadhyayula VKK, Deng S , Mitchell MC, Smith GF. Application of carbon nanotube technology for removal of contaminants in drinking water: A review. Science of the Total Environment. 2009; 408; 1–13.
47. Rostamian R, Behnejad H. A comparative adsorption study of sulfamethoxazole onto graphene and graphene oxide nanosheets through equilibrium, kinetic and thermodynamic modeling. Process Safety and Environmental Protection.2016;102;20-29.

48. Khaled A, Nem AE, El-Sikaily A, Abdelwahab O. Removal of Direct N Blue- 106 from artificial textile dye effluent using activated carbon from orange peel: adsorption isotherm and kinetic studies, J. Hazard. Mater. 2009: 165 ;100–110.
49. Gao Y, Li Y, Zhang L, Huang H, Hu J, Shah SM, Su X. Adsorption and removal of tetracycline antibiotics from aqueous solution by graphene oxide, J. Colloid. Interface Sci. 2012; 368; 540–546.